Results in Optics 2 (2021) 100025

Contents lists available at ScienceDirect

Results in Optics

journal homepage: www.elsevier.com/locate/rio

Exploring quantum-like turbulence with a two-component paraxial fluid of light

Nuno Azevedo Silva *, Tiago D. Ferreira, Ariel Guerreiro

INESC TEC, Centre for Applied Photonics, Rua do Campo Alegre 687, 4169-007 Porto, Portugal
Faculdade de Ciências da Universidade do Porto, Rua do Campo Alegre 687, 4169-007 Porto, Portugal

ARTICLE INFO

ABSTRACT

Fluids of light is an emergent topic in optical sciences that exploits the fluid-like properties of light to establish controllable and experimentally accessible physical analogues of quantum fluids. In this work we explore this concept to generate and probe quantum turbulence phenomena by using the fluid behavior of light propagating in a defocusing nonlinear media. The proposal presented makes use of orthogonal polarizations and incoherent beam interaction to establish a theoretical framework of an analogue two-component quantum fluid, a physical system that features a modified Bogoliubov-like dispersion relation for the perturbative excitations featuring regions of instability. We demonstrate that these unstable regions can be tuned by manipulating the relative angle of incidence between the two components, allowing to define an effective range of energy injection capable of exciting turbulent phenomena. Our numerical investigations confirm the theory and show evidence of direct and inverse turbulent cascades expected from weak wave turbulence theories. The works end on a discussion concerning its possible experimental realization, allowing the access to quantum turbulence in regimes beyond those previously explored by making use of the controllable aspects of tabletop fluids of light experiments.

1. Introduction

Turbulence is a non-equilibrium regime typically associated with hydrodynamic instabilities and characterized by complex dynamics at different length scales (Pope, 2001). Remaining as one of the open challenges in the physics of fluids, this phenomenon is widely reported in the most diverse systems and limits, ranging from classical to relativistic and quantum fluids (Pope, 2001; Micha and Tkachev, 2003; Nazarenko and Onorato, 2006). Concerning the latter, the experimental advances on Bose-Einstein Condensates (BEC) fostered in the last decades the research of quantum turbulence in a controllable manner (Nazarenko and Onorato, 2006; Kolmakov et al., 2014; Newell and Rumpf, 2011). Yet, experimental challenges like imaging or time-resolving vortex dynamics still undermine the access and exploration of a wider range of regimes in these systems (Kolmakov et al., 2014). In this context, the recent advent of quantum fluids of light (QFLs) brought novel opportunities in the field, promising versatile experimental approaches capable of providing valuable insight on open problems of quantum dynamics.

In short, QFLs are grounded on the hydrodynamic interpretation of the electromagnetic field which relates photons in an optical beam to an analogue quantum system with inter-particle interactions mediated by the nonlinear optical response of the media (Carusotto and Ciuti, 2013; Carusotto, 2014). The analogy can be established either in a cavity (Carusotto and Ciuti, 2013) or propagating geometries (Carusotto, 2014). The former – often called polariton or exciton–polariton fluids – is a successful approach in the observation of quantum-like dynamics, like superfluid behavior and vortex excitation (Amo et al., 2009; Sanvitto et al., 2010). Yet, as most of the experimental settings work with polaritons of short lifetimes, its dissipative and non-equilibrium character typically hurts the experimental reliability and pure quantum-like behavior applications at room temperature (Lerario et al., 2017). In its turn, QFLs in propagating geometries rely on a role exchange between time and the propagation distance: the beam density profile taken at consecutive planes along the propagation direction corresponds to snapshots of the analogue fluid system in successive time moments (Chiao and Boyce, 1999; Carusotto, 2014). Again, advances in this direction include observations of superfluid behavior, proving its potential as analogue quantum simulators (Carusotto, 2014; Larré and Carusotto, 2015; Silva et al., 2017). Compared against cavity configurations, these paraxial fluids of light are less susceptible to dissipation (Carusotto, 2014) and take advantage of tunable optical

* Corresponding author.
E-mail address: nuno.a.silva@inesctec.pt (N.A. Silva).

https://doi.org/10.1016/j.rio.2020.100025
Received 30 September 2020; Revised 13 November 2020; Accepted 14 November 2020

media and cutting-edge beam shaping techniques to achieve highly controllable experimental testbeds to explore quantum-like phenomena (Ferreira et al., 2018; Silva et al., 2017).

Regarding quantum turbulence, the possibility of using QFLs in propagating geometries was introduced recently (Rodrigues et al., 2020). In this setting, the problem is how to excite a turbulent regime using a specific range of energy injection at the experimental level. In the work of Rodrigues et al. (2020), the solution was to use coherent counter-propagating beams in nonlinear media, which lead to interference fringes that decay into what resembles a turbulent fluid. Yet, featuring only an ultra-quantum regime with a generation of a high density of vortex-antivortex pairs, clear evidence of the typical Kolmogorov energy cascades – a hallmark of turbulence – remained elusive, leaving open questions regarding the mechanism involved and if it is similar to the one that governs typical fluid turbulence.

In this work, we propose and investigate a different configuration to observe and probe quantum turbulence by making use of two orthogonal polarized beams propagating inside a defocusing nonlinear optical media of the Kerr-type. This approach, inspired in counter-streaming two-component BECs (Ishino et al., 2011), results in a different excitation mechanism, associated with a region of instability in the perturbative excitation spectrum that only appears above a velocity threshold which makes the system easier to play with at experimental level and capable of featuring the expected energy cascades. The paper is organized as follows: after an overview of the state-of-the-art in Sec. I, the Sec.II introduces the theoretical model to describe the envelope of each beam by means of two coupled Nonlinear Schrödinger equations(NLSE). Using perturbative techniques, we analyze the spectrum of small excitations on top of each fluid, obtaining a two-branch modified Bogoliubov dispersion relation featuring regions of instability that depend on the relative velocity between the two fluids. This excitation spectrum is confirmed through numerical simulations in Sec.III, showing evidence of the crossover between the superfluid and the turbulent dissipative regime. In Sec.IV we focus on the turbulent regime, reporting the dynamics involved and computing the compressible and incompressible part of the kinetic energy, observing the expected Komolgorov energy cascades. Finally, Sec.V presents our conclusions and discuss a possible experimental approach to the phenomena hereby described.

2. A two-component fluid of light

The starting point of our analysis is the model for the propagation of an electromagnetic field inside a nonlinear optical medium. In particular, we are interested in the dynamics of a monochromatic continuous wave beam inside a self-defocusing nonlinear medium, propagating along the z-axis and composed of two orthogonal polarized beams, i.e. $\boldsymbol{e}_{p1}\cdot\boldsymbol{e}_{p2}=0$ for $\boldsymbol{E}(\boldsymbol{r},t)=\left[E_1(\boldsymbol{r}_\perp,z,t)\boldsymbol{e}_{p1}+E_2(\boldsymbol{r}_\perp,z,t)\boldsymbol{e}_{p2}\right]\exp\left(i\boldsymbol{k}_0\boldsymbol{z}-i\omega_0 t\right)$, where E_i are the beam envelope functions and k_0 and ω_0 the wavenumber and frequency of the carrier wave respectively. In this scenario, taking the paraxial approximation on the Maxwell wave equation that assumes that the optical beam has a small incident angle in relation to the optical axis z (Kivshar and Agrawal, 2003), the mathematical model simplifies it to a set of coupled time-independent equations for each envelope given by

$$\frac{i}{k_0}\partial_z E_i+\frac{1}{2k_0^2}\nabla_\perp^2 E_i-n_2|E_i|^2E_i-\sigma n_2|E_{3-i}|^2E_i=0, \tag{1}$$

with $i=1,2$ where $n_2>0$ corresponds to the strength of the defocusing Kerr-type nonlinearity of the optical media and $\sigma\equiv 2/3$ is the coupling term associated with the incoherent interaction between the orthogonally polarized beams (Kivshar and Agrawal, 2003). The set of equation 1 corresponds to two coupled partial differential equations of the NLSE-type and is a model widely studied in contexts from Bose–Einstein condensates to optics, known to feature interesting phenomenology like dark-bright soliton solutions (Middelkamp et al., 2011; Carvalho et al., 1996; Kivshar and Agrawal, 2003), vortex dynamics (Law et al., 2010) and turbulence (Ishino et al., 2011, 2012, Tsubota et al., 2017), among others. In the context of fluids of light, the model shall correspond to a fluid composed of two components.

To understand how the analogy works, we shall now introduce the framework of fluids of light by applying the hydrodynamic interpretation for each optical beam. First, we transform the equation system 1 into a simpler adimensional form by performing an amplitude scaling $E_i'=E_i/E_0$ and coordinate scaling $\boldsymbol{r}'_\perp=\sqrt{\Delta n}\boldsymbol{k}_0\boldsymbol{r}_\perp$ and $z'=\Delta n k_0 z$,

$$i\partial_{z'}E_i'+\frac{1}{2}\nabla_\perp'^2E_i'-\left|E_i'\right|^2E_i'-\sigma\left|E_{3-i}'\right|^2E_i'=0, \tag{2}$$

with $\Delta n=n_2|E_0|^2$ corresponding to the refractive index change due to nonlinear effects. Subsequently, considering the Madelung transformation $E_i'=\sqrt{\rho_i}e^{i\phi}$ and dropping the primes, it is straightforward to derive from Eq. (1) the following set of hydrodynamic-like equations

$$\partial_z\rho_i+\nabla_\perp\cdot(\rho_i\boldsymbol{v}_i)=0 \tag{3}$$

$$\partial_z\boldsymbol{v}_i+(\boldsymbol{v}_i\cdot\nabla_\perp)\boldsymbol{v}_i=\nabla_\perp\left(\rho_i+\sigma\rho_{3-i}+\frac{\nabla_\perp^2\sqrt{\rho_i}}{2\sqrt{\rho_i}}\right) \tag{4}$$

for the density $\rho_i=\left|E_i'\right|^2$ and velocity field $\boldsymbol{v}_i=\nabla_\perp\phi$. Put in this way, the analogy behind fluids of light in propagating geometries is clearer: by replacing the role of time in common fluids with the propagation distance z, light behaves as fluid if we look at the local intensity as an analogue fluid density and at the gradient of the phase as an effective velocity. Furthermore, this gradient of phase is associated at $z=0$ with an incidence angle θ (see Fig. 1A), which from the conservation of the wavevector gives $\boldsymbol{v}_i=\sin\theta/\sqrt{\varepsilon\Delta n}$ with ε the linear dielectric constant of the medium. The last term of the velocity equation is commonly regarded as the quantum pressure or Bohm potential, and is responsible for the wave-like behavior and for the analogy with quantum fluids. In the subsequent sections, our approach will be based on the analogy at the mean-field level and on the Bogoliubov theory. Further investigation of the quantum fluid analogy involving field quantization and an operator formalism is left outside the scope of the paper but can be found in previous works (Larré and Carusotto, 2015; Carusotto and Ciuti, 2013).

2.1. Dispersion relation and instabilities

To get a general picture of the dynamics involved, we will now compute the perturbative excitation spectrum on top of constant-valued photon fluids in the case of counter-streaming configuration

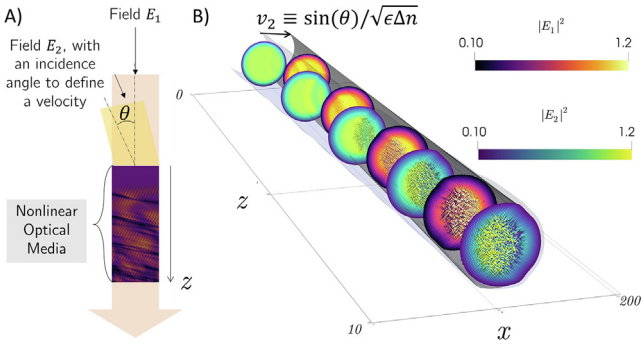

Fig. 1. Illustration of the two-component paraxial fluid of light in a counter-streaming configuration, as proposed in sec.II A of the main text. A) Entering the nonlinear optical media, one component has a velocity in relation to the other, which in experimental settings is achieved through the incidence angle θ. Typical results of numerical simulations in B) (2 + 1)-dimensional scenario, with the fluid-like behavior appreciated at successive consecutive planes along the propagation distance z.

(see Fig. 1). In order to do that, we consider that entering the nonlinear media the fluid component 2 is moving with velocity $\boldsymbol{v}$ along the x-axis – which corresponds in an experimental setting to an oblique angle of incidence $\theta = \arcsin\left(v\sqrt{\varepsilon\Delta n}\right)$ (see Fig. 1) – in relation to a fluid component 1 that has no effective velocity, perpendicularly incident on the nonlinear medium. In this case, it is straightforward to express the initial conditions as $E_1(\boldsymbol{r}_\perp, z=0) = \sqrt{\rho_1}$ and $E_2(\boldsymbol{r}_\perp, z=0) = \sqrt{\rho_2}e^{ivx}$. Taking a linear perturbative approach, the densities and velocities of each fluid can be expressed as

$$\rho_i = \rho_i + \delta\rho_i \tag{5}$$
$$\boldsymbol{v}_1 = \boldsymbol{\delta}v_1 \tag{6}$$
$$\boldsymbol{v}_2 = \boldsymbol{v} + \boldsymbol{\delta}v_2 \tag{7}$$

which substituted into the hydrodynamic equations, linearizing them and taking the Fourier transform, results in the matricial equation

$$\bar{M}\begin{pmatrix}\tilde{\delta\rho}_1\\ \tilde{\delta\rho}_2\end{pmatrix} = 0 \tag{8}$$

with

$$\bar{M} = \begin{pmatrix}L_1 & B\\ B & L_2\end{pmatrix} \tag{9}$$
$$L_i = -(\omega - \boldsymbol{k}_\perp\cdot\boldsymbol{v}_i)^2 + k_\perp^4/4 + \rho_i k_\perp^2 \tag{10}$$
$$B = \sigma\sqrt{\rho_1\rho_2}k_\perp^2, \tag{11}$$

and $\delta\tilde{\rho}_i(\boldsymbol{k}_\perp, \omega)$ standing for the Fourier transform both in the transverse space and propagation distance. The non-trivial solution requires $\det\left(\overline{M}\right) = 0$ and can be solved algebraically resulting on the dispersion relation $\omega(\boldsymbol{k}_\perp)$. For the sake of simplicity of the final expression, we for now on focus on the case of mass-balanced fluids $\rho_1 = \rho_2 = \rho$, for which the dispersion relation is

$$\left(\omega - \frac{\boldsymbol{v}\cdot\boldsymbol{k}_\perp}{2}\right)^2 = c^2k_\perp^2 + \frac{k_\perp^4 + k_\perp^2v^2}{4} \pm \sqrt{\left(\frac{k_\perp^4}{4} + c^2k_\perp^2\right)k_\perp^2v^2 + c^2k_\perp^4\sigma^2} \tag{12}$$

with the speed of sound defined as $c \equiv \sqrt{\rho}$. This dispersion relation corresponds to a modified two-branch Bogoliubov-like dispersion relation, typical of quantum fluids with superfluid properties. However, unlike the single-fluid dispersion relation, this collective excitation spectrum features a region of instability when the right-hand side of Eq. (12) becomes negative. Solving the resulting inequality for $\boldsymbol{v}$ it is straightforward to prove that instability occurs for a velocity value above a critical velocity

$$v > 2c\sqrt{1-\sigma} \equiv v_c. \tag{13}$$

Put in this way, we identify 3 distinct regimes: (i) for $v < v_c$ there is no region of instability (see Fig. 2A); (ii) for $v_c < v < 2c\sqrt{1+\sigma}$ there is a region of instability for small wavenumbers $0 < k_\perp < k_+$ with $k_+ \equiv \sqrt{v^2 - v_c^2}$(see Fig. 2C); and (iii) for $v > 2c\sqrt{1+\sigma}$, which features a region of instability in the limited range $k_- < k_\perp < k_+$ with $k_- \equiv \sqrt{v^2 - 4c^2(1+\sigma)}$ (see Fig. 2D).

To prove the existence of this dispersion relation we performed numerical simulations, adapting an oceanographic-inspired methodology in (1 + 1)-dimensional settings (Kumar et al., 2017). In short, the idea is that starting with an input field consisting of an constant background plus a random small amplitude white noise Δ, i.e.

$$E_1(x,0) = \sqrt{n} \text{ and } E_2(x,0) = \sqrt{n}e^{ivx} + \Delta \tag{14}$$

allows to excite a large spectrum of small amplitude elementary excitations in $k_\perp$ that shall evolve according to 12. To retrieve the dispersion relation, the coupled NLSEs are simulated up to a final propagation distance z_f, recording the data for a set of values for z, and finally taking the Fourier transform of the entire data both in the transverse dimension and propagation distance.

Using a standard SSFM methodology (Silva et al., 2017), we performed simulations of Eq. (1) with $\rho = 1, \sigma = 2/3$ and $z_f = 2000$ for different values of $\mathcal{V}$, obtaining the results presented in Figure 2. As seen, the results verify the predictions above, which also validates the methodology. On one hand, looking at Fig. 2E and F we see that there is no region of instability, with the higher values of the intensity spectrum – represented by the light-shaded areas of the density plot – showing the predicted dispersion relation of Eq. (12) – represented by dashed lines. On the other hand, for $v_c < v < 2c\sqrt{1+\sigma}$ depicted in Fig. 2G, we still see an agreement between the predicted curves and those observed, but also it should be noted the region of instability that is developing at small wavenumbers $0 < k_\perp < k_+$. In spite the appearance of nonlinear processes, similar results are still observed for the third regime described above, confirming the possibility to excite a limited unstable region $k_- < k_\perp < k_+$ by simply increasing the relative velocity.

2.2. Dissipative motion and energy transfer

In the dynamical regimes described, one of the interesting questions is if and in what conditions does energy transfer between the two components of the fluid occurs. For that, we focus on the momentum of each component,

$$\boldsymbol{J}_i = \frac{1}{2i}\int d\boldsymbol{r}_\perp\left(E_i^*\nabla E_i - E_i\nabla E_i^*\right) \tag{15}$$

which under the hydrodynamic formulation can be expressed as $\boldsymbol{J}_i = \rho_i\boldsymbol{v}_i$. Exchange of momentum shall occur when $\delta\boldsymbol{J}_i = \delta\rho_i\boldsymbol{v}_i + \rho_i\boldsymbol{\delta}v_i \neq 0$ (Takeuchi et al., 2010), but still as to respect the additional total momentum conservation law $\delta\boldsymbol{J}_1 + \delta\boldsymbol{J}_2 = 0$ of a closed system.

Taking the first order of perturbation, we first recast Eq. (8) into a relation between the perturbation for each component as

$$\tilde{\delta\rho}_2 = -L_1\tilde{\delta\rho}_1/B. \tag{16}$$

Noting that from the mass conservation equation an additional condition can be obtained as

$$(\omega - \boldsymbol{v}_i\cdot\boldsymbol{k}_\perp)\delta\rho_i = \rho_i\boldsymbol{k}_\perp\cdot\tilde{\boldsymbol{\delta}v}_i, \tag{17}$$

the conservation of momentum results in (1 + 1)-dimensional settings into a condition

$$\omega(B - L_1)\tilde{\delta\rho}_1 = 0, \tag{18}$$

which is non-trivially satisfied for $B = L_1$. Imposing the computed dispersion relation, it is easy to obtain that the existence of real solutions in k require $v > v_c$, which associates the existence of instabilities in the excitation spectrum with the dissipative motion regime and energy transfer between the two components of the fluid (Ishino et al., 2011; Takeuchi et al., 2010; Ishino et al., 2012; Tsubota et al., 2017). These predictions align with the literature and were confirmed numerically computing the momentum using Eq. (15) for the same simulations of the previous section (see Fig. 3).

3. Turbulent regimes and energy cascades

For small propagation distances, the dynamics of the unstable modes can still be described within the Bogoliubov excitation framework. Yet, the exponential amplification of these modes eventually breaks the perturbative approach. This process can be observed by inspection of Fig. 4 that represents the amplitude of the excitation modes of the simulations of the previous sections in function of the wavenumber for different propagation distances and relative velocities. While for $v < v_c$ we see no significant variation of the amplitude across the spectrum, the cases of $v > v_c$ show a clear amplification process. As seen, the amplification first occurs in the predicted unstable k-range, defining a limited interval of energy injection for $v > 2c\sqrt{1+\sigma}$

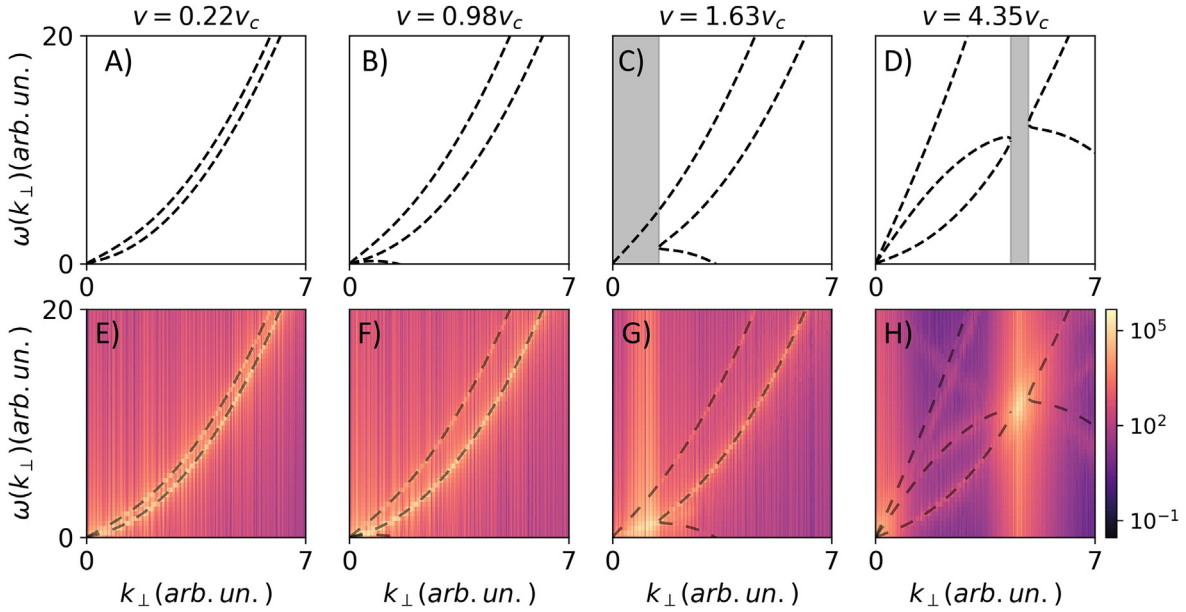

Fig. 2. Two-branch Bogoliubov collective excitation spectrum and instability regions (shaded regions in the top panel) for different values of relative velocity. Subfigures correspond to results obtained theoretically from a linear perturbative approach(top panel, A–D) and numerically using the simulation strategy described in the main text (bottom panel, E–H).

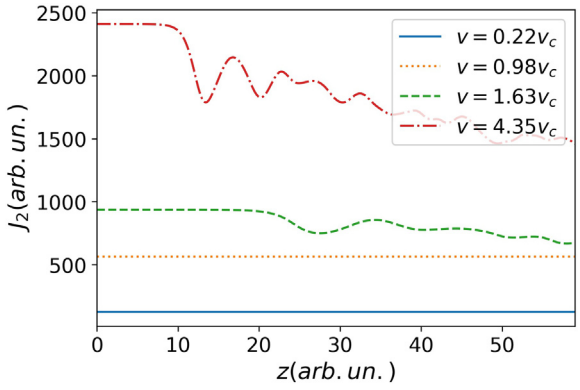

Fig. 3. Momentum of fluid component E_2 computed from Eq. (15) in function of the propagation distance for different relative velocities, exhibiting a dissipationless regime for $v < v_c$ in opposition to the dissipative one for $v > v_c$.

as discussed before. It is then safe to assume that at least for relatively small propagation distances, the unstable region of the Bogoliubov spectrum defines a range for the energy injected into the system, a range that is important to generate turbulent phenomena and crucial for the observation of associated energy cascades. Note that at the experimental level, this range can be tuned by simply modifying the incidence angle of one optical beam, which can be a major advantage for exploring quantum-turbulence.

For larger propagation distances, nonlinear effects come into play, allowing to excite modes at different scales that precede the turbulent regime. In theory, energy cascades develop at this stage, corresponding to the transference of kinetic energy between different dynamical scales. In quantum fluids, energy cascades were reported to exist both in the direct - flowing towards smaller scales, i.e. larger wavenumbers – and inverse – flowing towards larger ones, i.e. smaller wavenumbers – directions, with characteristic power-law scalings associated with distinct phenomenology (Kolmakov et al., 2014; Newell and Rumpf, 2011; Reeves et al., 2012; Numasato et al., 2010; Horng et al.,

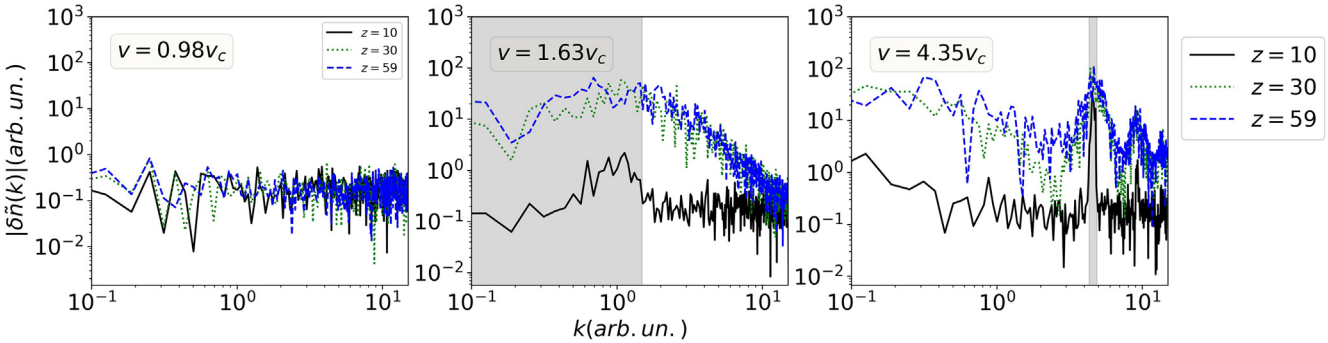

Fig. 4. Fourier spectrum computed in the transverse dimensions for different propagation distances and varying relative velocities. The shaded region represent the unstable range of the dispersion relation as discussed in sec. II.

2009). On one hand, the direct enstrophy cascades are typically related to the generation of unstable line patterns that later decay into vortices (Dyachenko et al., 1992; Numasato et al., 2010). On the other hand, the existence of inverse cascades in quantum fluids is more debatable and known to occur only under specific conditions, with evidence that associate it with self-organization phenomena occurring at large scales (Horng et al., 2009; Tsubota et al., 2017).

To investigate the existence of such turbulence signature we now focus on the dynamics of light fluids in (2 + 1)-dimensional systems, using for that purpose two flat-top supergaussian beams as initial conditions for each fluid component(see Figure1B), i.e.

$$E_1(x,y,z=0) = e^{-\left((x-x_1)^4+(y-y_1)^4\right)/w^4} \tag{19}$$

$$E_2(x,y,z=0) = e^{-\left((x-x_2)^4+(y-y_2)^4\right)/w^4 - ivx} + \Delta. \tag{20}$$

Using the same numerical tools, we solved the equation system 1 on a two dimensional box of 1024×1024 points, considering the beams centered at $(x_1, y_1) = (205, 105)$ and $(x_2, y_2) = (120, 105)$ and explored the results for various values of v. To avoid a significant beam divergence within the total propagation distance $z_f = 40$ we used $w = 500$. Typical results of these simulations are represented in Fig. 5, qualitatively suggesting the existence of turbulent phenomena with evidence of the aforementioned enstrophy mechanism, the generation of unstable line patterns that later decay into vortices.

Regarding energy cascades, the Kolmogorov–Zakharov weak wave turbulence theory predicts the cascades to occur in the incompressible part of the kinetic energy (Kolmakov et al., 2014; Newell and Rumpf, 2011; Numasato et al., 2010). This means that a complete numerical investigation requires the decomposition of the density-weighted velocity into its incompressible and compressible components,

$$\boldsymbol{u}_i(\boldsymbol{r}_\perp, z) = \sqrt{\rho}\boldsymbol{v}_i = \boldsymbol{u}_i^I + \boldsymbol{u}_i^C \tag{21}$$

satisfying $\nabla \cdot \boldsymbol{u}_i^I = 0$ and $\nabla \times \boldsymbol{u}_i^C = 0$. As cascades occur in momentum space, we take the Fourier transform in the transverse space which simplifies the process of separating the two components to computing the formulas (Koniakhin et al., 2020)

$$\tilde{\boldsymbol{u}}_{i\beta}^I(\boldsymbol{k}, z) = \sum_{\alpha=x,y}\left(\delta_{\alpha,\beta} - \frac{k_\alpha k_\beta}{k^2}\right)\tilde{\boldsymbol{u}}_{i\alpha} \tag{22}$$

$$\tilde{\boldsymbol{u}}_{i\beta}^C(\boldsymbol{k}, z) = \sum_{\alpha=x,y}\frac{k_\alpha k_\beta}{k^2}\tilde{\boldsymbol{u}}_{i\alpha}. \tag{23}$$

Under these definitions the kinetic energy is decomposed as $E_k = E_k^I + E_k^C$, which integrating over the angular dependence gives each spectral energy density as

$$E_k^I(k,z) = \frac{k_\perp}{2}\int d\theta\left(\left|\tilde{\boldsymbol{u}}_1^I(\boldsymbol{k},z)\right|^2 + \left|\tilde{\boldsymbol{u}}_2^I(\boldsymbol{k},z)\right|^2\right) \tag{24}$$

$$E_k^C(k,z) = \frac{k_\perp}{2}\int d\theta\left(\left|\tilde{\boldsymbol{u}}_1^C(\boldsymbol{k},z)\right|^2 + \left|\tilde{\boldsymbol{u}}_2^C(\boldsymbol{k},z)\right|^2\right) \tag{25}$$

in the momentum space. Following this procedure, we were able to compute each energy spectra for the simulation described above, obtaining the results presented in Fig. 6.

Both cascades predicted by the Komolgorov theory can be identified upon inspection of Fig. 6. For larger wavenumbers, above the energy injection range, an enstrophy cascade forms decaying with a k^{-4} power law as expected from the Saffman theory, illustrating the energy transfer from larger to smaller scales (Horng et al., 2009). For even smaller scales, the decay starts to deviate from this regime as the system is non-dissipative and features no energy sinks. On the other side, an inverse cascade forms just above the energy injection rate into larger scales, following the predicted $k^{-5/3}$ power law (Horng et al., 2009; Reeves et al., 2012). This cascade becomes less evident approaching smaller wavenumbers, which can be associated with the finite size of the flat-top beams and their inhomogeneities. Nevertheless, in previous approaches with paraxial fluids of light, these regimes were not successfully identified (Rodrigues et al., 2020), which demonstrates the merit of our two-fluid proposal by allowing finer control of the instability mechanism.

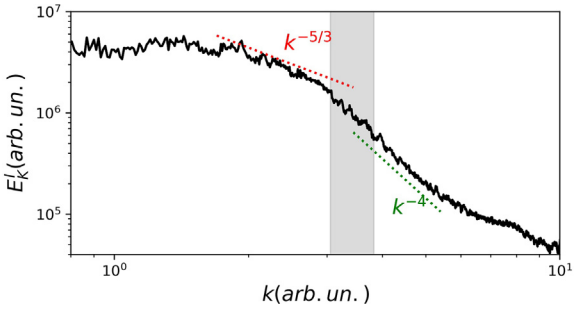

Fig. 6. Incompressible kinetic energy spectra obtained from the analysis of the simulation described in the main text and represented in figure 5 at $z = 15$. In addition, we represented the expected power law tendencies as described in the main text, as well as the region of instability which corresponds to the energy injection range.

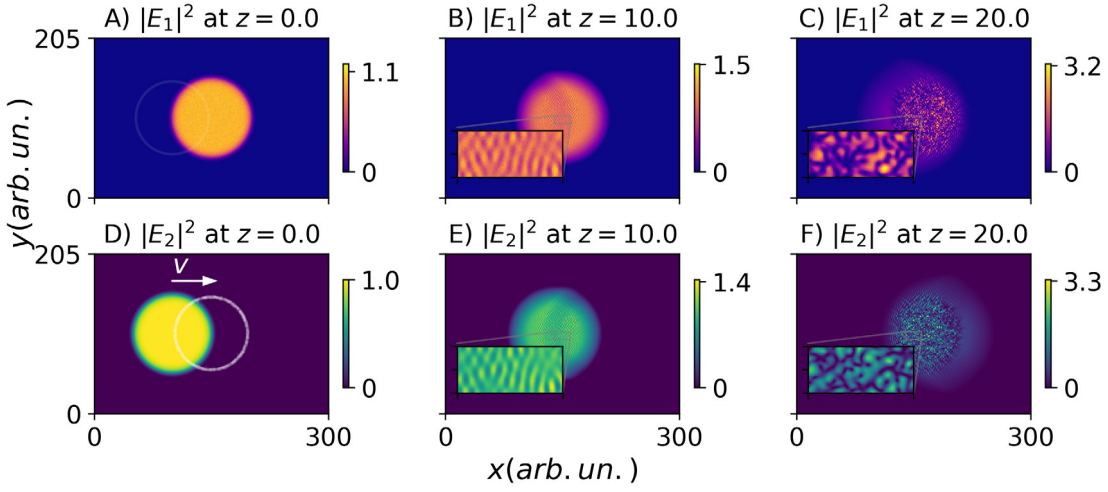

Fig. 5. Numerical results of the simulation of two colliding flat-top beams as described in the main text for a relative velocity $v = 4$. Top and bottom panels correspond to the first E_1 and second E_2 fluid components, respectively.

4. Conclusion

Probing turbulence in controllable experimental settings is crucial for the development of a complete and robust picture of such complex phenomena. In particular for turbulence in quantum fluids, the usual experimental approach explores Bose–Einstein condensates, which is limited by various experimental challenges from imaging to the dissipative dynamics that deviates the system from a pure quantum behavior (Lerario et al., 2017). In this context, this work proposes an alternative setting exploiting fluids of light, an emerging concept in optical analogues that explores the fluid-like properties of light propagating inside a defocusing nonlinear optical media to probe quantum-like behavior.

Focusing on the dynamics of two orthogonal polarized beams interacting incoherently through the nonlinear optical properties of the media, we established a theoretical framework analogue to a two-component quantum fluid using the hydrodynamic interpretation of light. Through a perturbative approach we have shown that if the two beams cross at an angle, the collective excitation spectrum deviates from the typical Bogoliubov dispersion relation. In particular, for a velocity above a critical value, the two-branched dispersion relation features a region of instability which we prove to be associated with a dissipative regime and momentum transfer between the two beams. Numerical simulations show that this instability precedes a turbulent regime and corresponds to an effective energy injection range. This finding allowed observing the theoretically predicted direct and indirect energy cascades featuring the k^{-4} and $k^{-5/3}$ power laws, respectively.

Finally, regarding a possible experimental realization, studies involving fluids of light in propagating geometries have been focused on the use of nonlinear crystals, nonlocal fluids, and atomic vapors in near-resonant regimes (Michel et al., 2018; Ferreira et al., 2018; Fontaine et al., 2018). In particular, the higher nonlinear strength and versatility of the later has been explored successfully recently and would be particularly interesting in the context of quantum turbulence, by allowing to assess the quantum-like behavior in typical propagating distances around the millimeter scale (Fontaine et al., 2018; Rodrigues et al., 2020). In this context, the proposal in this work can leverage the state-of-the-art and be realized adapting a typical experiment with hot rubidium vapors with a set of tunable laser sources, with a CCD sensor to measure the intensity pattern at the near-field and an interference with a reference plane wave to compute the equivalent fluid velocity and assess the energy cascades. With a nonlinear refractive index change around $\Delta n \approx 10^{-5}$, results from section III can be recreated in the laboratory with vapor cell of around 1 cm in the transverse dimensions and a total length below 20 cm, and the necessary incident angles are of the order of 10^{-2} rad which is well within the limits of validity for the paraxial approximation. These quantities are reasonable from an experimental point of view, which probes the potential of the framework to open an innovative path towards experimental investigations on quantum turbulence, exploiting its controllable aspects to inspire research that can go beyond that assessed using the typical BEC framework (Tsubota et al., 2017; Kolmakov et al., 2014).

CRediT authorship contribution statement

Nuno Azevedo Silva: Conceptualization, Software, Formal analysis, Writing - original draft. **Tiago D. Ferreira:** Software, Writing - review & editing. **Ariel Guerreiro:** Writing - review & editing, Project administration.

Declaration of Competing Interest

The authors declare that they have no known competing financial interests or personal relationships that could have appeared to influence the work reported in this paper.

Acknowledgments

This work is financed by the European Regional Development Fund (ERDF) through the Operational Programme for Competitiveness and Internationalisation, COMPETE 2020 Programme, and by National Funds through the FCT Fundação para a Ciência e a Tecnologia (Portuguese Foundation for Science and Technology), within Project No. POCI-01-0145-FEDER-032257, as well as by the North Portugal Regional Operational Programme (NORTE 2020), under the PORTUGAL 2020 Partnership Agreement. Also, the authors acknowledge the financial support of the project “Quantum Fluids of Light in Hot Atomic Vapors”, supported by FCT in collaboration with the Ministry of Education, Science and Technological Development of the Republic of Serbia. T.D.F. is supported by Fundação para a Ciência e a Tecnologia through Grant No. SFRH/BD/145119/2019. N.A.S and A.G. also acknowledge the Texas Advanced Computing Center (TACC) at The University of Texas at Austin for providing visualization resources that have contributed to the research results reported within this paper.

References

Pope, S.B., 2001. Turbulent Flows.
Micha, R., Tkachev, I.I., 2003. Physical Review Letters 90, 121301.
Nazarenko, S., Onorato, M., 2006. Physica D: Nonlinear Phenomena 219, 1.
Kolmakov, G.V., McClintock, P.V.E., Nazarenko, S.V., 2014. Proceedings of the National Academy of Sciences 111, 4727.
Newell, A.C., Rumpf, B., 2011. Annual Review of Fluid Mechanics 43, 59.
Carusotto, I., Ciuti, C., 2013. Reviews of Modern Physics 85, 299.
Carusotto, I., 2014. Proceedings of the Royal Society A: Mathematical, Physical and Engineering Sciences 470, 20140320.
Amo, A., Lefrère, J., Pigeon, S., Adrados, C., Ciuti, C., Carusotto, I., Houdré, R., Giacobino, E., Bramati, A., 2009. Nature Physics 5, 805.
Sanvitto, D., Marchetti, F., Szymańska, M., Tosi, G., Baudisch, M., Laussy, F.P., Krizhanovskii, D., Skolnick, M., Marrucci, L., Lemaitre, A., et al, 2010. Nature Physics 6, 527.
Lerario, G., Fieramosca, A., Barachati, F., Ballarini, D., Daskalakis, K.S., Dominici, L., De Giorgi, M., Maier, S.A., Gigli, G., Kéna-Cohen, S., et al, 2017. Nature Physics 13, 837.
Chiao, R.Y., Boyce, J., 1999. Physical Review A 60, 4114.
Larré, P.-É., Carusotto, I., 2015. Physical Review A 91, 053809.
Silva, N.A., Mendonça, J., Guerreiro, A., 2017. JOSA B 34, 2220.
Ferreira, T.D., Silva, N.A., Guerreiro, A., 2018. Physical Review A 98, 023825.
Rodrigues, J.D., Mendonça, J.T., Terças, H., 2020. Physical Review A 101, 043810.
Ishino, S., Tsubota, M., Takeuchi, H., 2011. Physical Review A 83, 063602.
Kivshar, Y.S., Agrawal, G.P., 2003. Optical solitons: from fibers to photonic crystals. Academic Press.
Middelkamp, S., Chang, J., Hamner, C., Carretero-González, R., Kevrekidis, P., Achilleos, V., Frantzeskakis, D., Schmelcher, P., Engels, P., 2011. Physics Letters A 375, 642.
Carvalho, M., Singh, S., Christodoulides, D., Joseph, R., 1996. Physical Review E 53, R53.
Law, K., Kevrekidis, P., Tuckerman, L.S., 2010. Physical Review Letters 105, 160405.
Ishino, S., Tsubota, M., Takeuchi, H., 2012. Journal of Physics. Conference Series (Online) 400.
Tsubota, M., Fujimoto, K., Yui, S., 2017. Journal of Low Temperature Physics 188, 119.
Larré, P.-É., Carusotto, I., 2015. Physical Review A 92, 043802.
Kumar, S., Perego, A., Staliunas, K., 2017. Physical Review Letters 118, 044103.
Takeuchi, H., Ishino, S., Tsubota, M., 2010. Physical Review Letters 105, 205301.
Reeves, M., Anderson, B.P., Bradley, A., 2012. Physical Review A 86, 053621.
Numasato, R., Tsubota, M., Lvov, V.S., 2010. Physical Review A 81, 063630.
Horng, T.-L., Hsueh, C.-H., Su, S.-W., Kao, Y.-M., Gou, S.-C., 2009. Physical Review A 80, 023618.
Dyachenko, S., Newell, A.C., Pushkarev, A., Zakharov, V.E., 1992. Physica D: Nonlinear Phenomena 57, 96.
Koniakhin, S., Bleu, O., Malpuech, G., Solnyshkov, D., 2020. Chaos. Solitons & Fractals 132, 109574.
Michel, C., Boughdad, O., Albert, M., Larré, P.-É., Bellec, M., 2018. Nature Communications 9, 1.
Fontaine, Q., Bienaimé, T., Pigeon, S., Giacobino, E., Bramati, A., Glorieux, Q., 2018. Physical Review Letters 121, 183604.